

Synthesis of Graphene Oxide (GO) by Modified Hummers Method and Its Thermal Reduction to Obtain Reduced Graphene Oxide (rGO)*

Syed Nasimul Alam, Nidhi Sharma, Lailesh Kumar

Department of Metallurgical and Materials Engineering, National Institute of Technology Rourkela, Rourkela, India
Email: nasimulalam@yahoo.com, syedn@nitrkl.ac.in

How to cite this paper: Alam, S.N., Sharma, N. and Kumar, L. (2017) Synthesis of Graphene Oxide (GO) by Modified Hummers Method and Its Thermal Reduction to Obtain Reduced Graphene Oxide (rGO). *Graphene*, 6, 1-18.
<http://dx.doi.org/10.4236/graphene.2017.61001>

Received: November 3, 2016

Accepted: January 7, 2017

Published: January 10, 2017

Copyright © 2017 by authors and Scientific Research Publishing Inc.
This work is licensed under the Creative Commons Attribution International License (CC BY 4.0).

<http://creativecommons.org/licenses/by/4.0/>



Open Access

Abstract

Over the span of years, improvements over various synthesis methods of graphene are constantly pursued to provide safer and more effective alternatives. Though the extraction of graphene through Hummers method is one of the oldest techniques yet it is one of the most suitable methods for the formation of bulk graphene. Graphene can be obtained in the form of reduced Graphite oxide, sometimes also referred as Graphene oxide. The effectiveness of this oxidation process can be evaluated by the magnitude of carbon/oxygen ratio of the obtained graphene. Here, graphene oxide (GO) was prepared by oxidizing the purified natural flake graphite (NFG) by a modified Hummers method. The attempts have been made to synthesize GO having few layers by using a modified Hummers method where the amount of NaNO_3 has been decreased, and the amount of KMnO_4 is increased. The reaction has been performed in a 9:1 (by volume) mixture of $\text{H}_2\text{SO}_4/\text{H}_3\text{PO}_4$. This modification is successful in increasing the reaction yield and reducing the toxic gas evolution while using a varied proportion of KMnO_4 and H_2SO_4 as those required by Hummers method. A new component of $\text{K}_2\text{S}_2\text{O}_8$ has been introduced to the reaction system to maintain the pH value. Reduced graphene oxide (rGO) was thereafter extracted by thermal modification of GO. Here, GO has been used as a precursor for graphene synthesis by thermal reduction processes. The results of FTIR and Raman spectroscopy analysis show that the NFG when oxidized by strong oxidants like KMnO_4 and NaNO_3 , introduced oxygen atoms into the graphite layers and formed bonds like C=O, C-H, COOH and C-O-C with the carbon atoms in the graphite layers. The structure and morphology of both GO and rGO were analyzed using X-ray diffraction (XRD), scanning electron microscopy (SEM), high-resolution transmission electron microscopy (HR-TEM), Fourier transform infrared spectroscopy (FTIR), ultraviolet-visible spectroscopy, Raman spectroscopy, Brunauer-Emmett-Teller (BET) surface area analysis and differential scanning calorimetry (DSC) and thermogravimetric analysis (TGA).

*Synthesis of GO by Modified Hummers Method.

Keywords

Graphene Oxide (GO), Reduced Graphene Oxide (rGO), Exfoliated Graphite Nanoplatelets (xGnP)

1. Introduction

Study of carbon nanostructures is very extensive due to their unmatched properties and numerous applications. Among the various species of carbon, graphene is one of the most talked about in the present era due to its remarkably excellent properties [1] [2]. Graphene has excellent electronic, mechanical and thermal properties. Graphene has a specific surface area of 2620 m²/g. It has a Young's modulus of 1 TPa and intrinsic strength of 130 GPa. It has a very high electronic conductivity at room temperature, and its electron mobility is 2.5×10^5 cm²/Vs. Its thermal conductivity is around 3000 Wm/K. Graphene has a unique two-dimensional structure consisting of a single atomic layer of sp₂ hybridized carbon atoms. Single-layer transferable graphene nanosheets were first obtained by mechanical exfoliation (Scotch-tape method) of bulk graphite [3] and by epitaxial chemical vapour deposition [4]. Though these routes are preferred for the precise device assembly, yet they are not suitable for the bulk production of graphene and not used for its large scale manufacturing. The mechanical exfoliation techniques used to obtain graphene nanosheets are not effective for large scale synthesis, so scalable synthesis approaches from structurally similar compounds are of great scientific interest. Scalability is an important factor for the synthesis of graphene, and one of the most popular approaches towards graphite exfoliation is the use of strong oxidizing agents to obtain Graphene oxide (GO), a nonconductive hydrophilic carbon material [5] [6]. Chemical means are a practical approach for the bulk scale synthesis of graphene [7]. Although the exact structure of GO is difficult to determine, it is clear that for GO the previously contiguous aromatic lattice of graphene is interrupted by epoxides, alcohols, ketones, and carboxylic groups. The interruption of the lattice is reflected by an increase in interlayer spacing from 0.335 nm for graphite to more than 0.625 nm for GO [8] [9] [10]. GO can be readily synthesized by the oxidation of the natural flake graphite (NFG) powder. GO is of great interest due to its low cost, easy access, and widespread ability to convert to graphene. The most common source of graphite is the flake graphite. Flake graphite is a naturally occurring mineral that is purified by removing the heteroatomic contamination. Brodie first demonstrated the synthesis of GO in 1859 by adding a portion of potassium chlorate to a slurry of graphite in fuming nitric acid [11]. In 1898, Staudenmaier improved on this protocol by using a mixture of concentrated sulfuric acid and fuming nitric acid followed by gradual addition of chlorate to the reaction mixture. This small change in the procedure provided a simple and revised protocol for the production of highly oxidized GO [12]. In 1958, Hummers reported an alternative method for the synthesis of graphene oxide by using KMnO₄ and NaNO₃ in concentrated H₂SO₄ [13]. GO prepared by this method could be used for preparing large graphitic films [14].

In the present work, oxidation has been done using the modified Hummers method

and thereafter GO has been reduced thermally in order to obtain graphene. GO is synthesized by the oxidative treatment of graphite by one of the principle methods developed by Brodie, Hummers or Staudenmaier because it has several advantages over the present reduction techniques. Firstly, the reaction can be completed within a few hours. Secondly, KClO_3 was replaced by KMnO_4 to improve the reaction safety, avoiding the evolution of explosive ClO_2 , KClO_3 . Thirdly, the use of NaNO_3 instead of fuming HNO_3 eliminates the formation of acid fog. Hummers method has attracted a large attention because of its high efficiency and satisfying reaction safety. However, it still has a few drawbacks. For instance, the oxidation procedure releases toxic gasses such as NO_2 and N_2O_4 and also the residual Na^+ and NO_3^- ions are difficult to be removed from the waste water formed from the processes of synthesizing and purifying GO. The modification used in present work is successful in increasing the reaction product and further reducing evolution of the toxic gas while using a varied proportion of KMnO_4 and H_2SO_4 as those required by Hummers method. The substantial use of $\text{K}_2\text{S}_2\text{O}_8$ maintains the pH value continuously during the reaction. Although it is very difficult to determine the exact structure of GO, it is known that in GO the contiguous aromatic lattice in graphene is interrupted by the various functional groups. GO has a similar layered structure as that of graphite, but the plane of carbon atoms in GO is heavily decorated by oxygen-containing groups, which not only expand the interlayer distance but also make the atomic-thick layers hydrophilic. As a result, these oxidized layers can be exfoliated under moderate ultrasonication. If exfoliated sheets contain only one or few layers of carbon atoms like graphene, these sheets are named graphene oxide (GO). These graphene oxides have important applications in areas related to transparent conductive film, composite materials, solar energy and biomedical applications. Hygroscopicity and dispersibility are the main properties of GO. **Figure 1(a)** shows the structure of a single layer graphene and **Figure 1(b)** shows the structure of graphene oxide. GO sheet can be considered as the combined structure of oxygen-containing functional groups, such as C-O, C=O and -OH that has been supported on the surface of a single layer graphene. As a result of the addition of oxygen-containing functional groups both the structure and the properties of GO changes. The oxidation process produces structural defects which shift the physical properties of GO away from that of

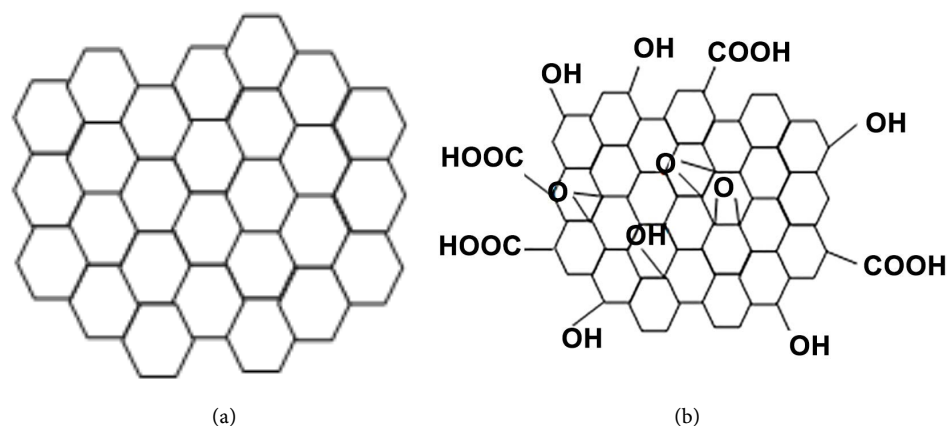


Figure 1. Schematic structure of (a) a single graphene sheet; (b) graphene oxide (GO).

pure graphene. However, the presence of the oxygen-containing functional groups also makes GO strongly hydrophilic as a result of which GO can be dispersed in several solvents like water [15]-[21].

2. Experimental Method

Graphene oxide (GO) has been initially prepared by a modified Hummers method. Subsequently reduced graphene oxide (rGO) having few layer graphene is extracted from GO by the thermal reduction of GO. Natural flake graphite (NFG) was procured from LOBA Chemie India having a mean size of 60 mesh and purity of 98%. Sulfuric acid (H_2SO_4) and phosphorous pentoxide (P_2O_5) were procured from Merck India. All reagents used were of analytical grade and had the highest commercially available purity. A mixture of 4 gm of NFG, 12 ml H_2SO_4 and 8 gm of P_2O_5 was prepared. The solution was subjected to magnetic stirring for a period of 6 h. 12 ml of H_2SO_4 was again added to the filtrate along with 8 gm of $\text{K}_2\text{S}_2\text{O}_8$. This mixture was magnetically stirred for 6 h. After cooling the mixture to the room temperature, it was diluted with 300 ml of distilled water. The filtrate was then dried overnight in air and later heated in a muffle furnace in air at 60°C for 2 h in order to remove the moisture. 2 gm of the pre-oxidised graphite powder is then added to the mixture of 92 ml H_2SO_4 and 12 gm KMnO_4 under continuous stirring in a water bath. 2 gm of NaNO_3 is then added to the solution after 15 mins. This solution is then stirred at room temperature for 2 h. Later 200 ml of distilled water is added to the solution and stirred for 15 mins. 10 ml of 30% of H_2O_2 and 560 ml of distilled water is added to the solution. The filtrate obtained is washed with HCl (10%). The brown suspension obtained is heated in a muffle furnace for 30 mins at 60°C and then allowed to cool overnight in air. The brown dispersion is dialyzed extensively to remove residual metallic ions and acids with distilled water for 1 week. Finally, the filtrate was air dried overnight and sonicated for 5 with H_2O_2 . The yellow-brown residual powder was washed with warm water for upto 3 times to remove the impurities. The dry GO powder is finally obtained after heating the filtrate at 60°C for 4 h. To obtain rGO from GO, 100 mg of the dried GO powder is taken in an empty beaker. The beaker was covered with aluminium foil that had many punched pores and was placed on a hot plate set at 350°C for 10 mins in a hood. The resulting black powder of rGO was then collected from the beaker. **Figure 2** shows the various steps that have been undertaken for the synthesis of rGO from NFG.

Fourier transform infrared (FTIR) spectra of the samples were recorded on an IR-Prestige-21 Shimadzu spectrophotometer using KBr as the mulling agent. X-ray diffraction analysis (XRD) of powders were carried out on a Panalytical PW 3040 X'Pert MPD X-ray diffractometer using Cu K_α radiation ($\lambda = 1.541 \text{ \AA}$). The morphologies of the samples were observed under a JEOL JSM-6480LV scanning electron microscope (SEM). A Nova NanoSEM 450/FEI field emission scanning electron microscope (FESEM) was also used to analyze the various samples. Micro-Raman measurements were made with a T64000 Jobin Yvon Horiba system. Differential scanning calorimetry (DSC) and thermogravimetric analysis (TGA) was done in a Netzsch STA 409C Simultaneous Thermal Analyzer at a heating rate of $10^\circ\text{C}/\text{min}$ in Ar atmosphere to determine the thermal stability of the various samples. A Quantachrome, USA, BET (Brunauer-

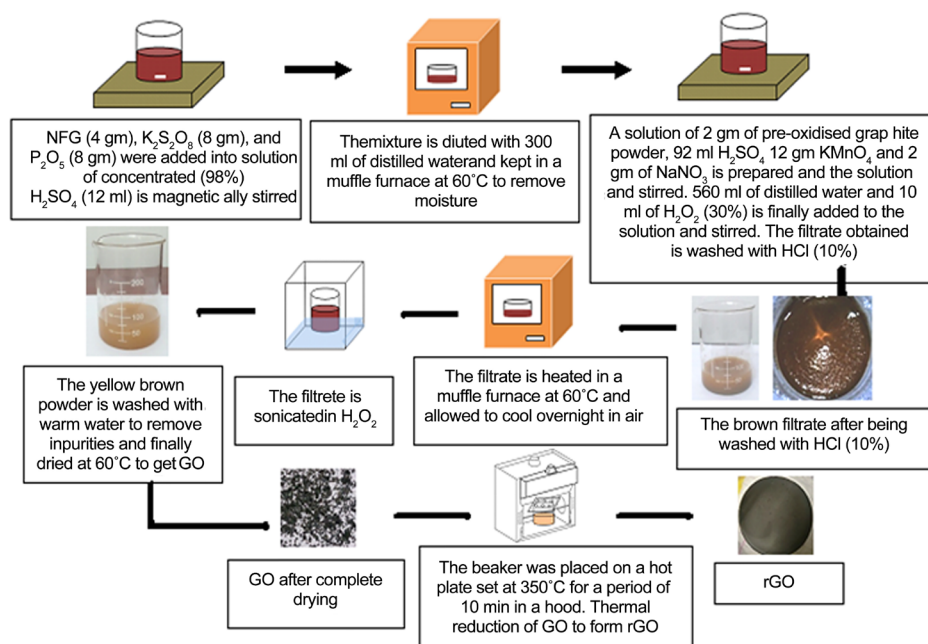


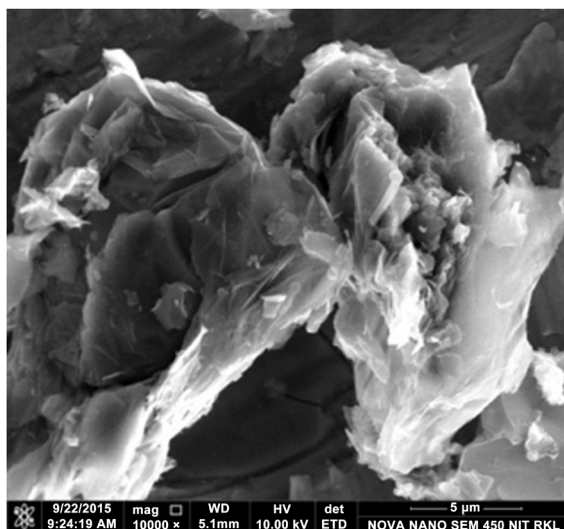
Figure 2. Schematic diagram showing the steps undertaken for the synthesis of GO and rGO.

Emmet-Teller) surface area analyzer was used for surface area and pores size measurements by N_2 adsorption-desorption analysis. BET analysis provides precise, specific surface area evaluation of materials by N_2 multilayer adsorption measured as a function of relative pressure and can also be employed to determine pore area and specific pore volume using adsorption and desorption techniques. Atomic force microscopy (AFM) analysis was done using a Veeco/849-012-711 Scanning probe microscope (SPM).

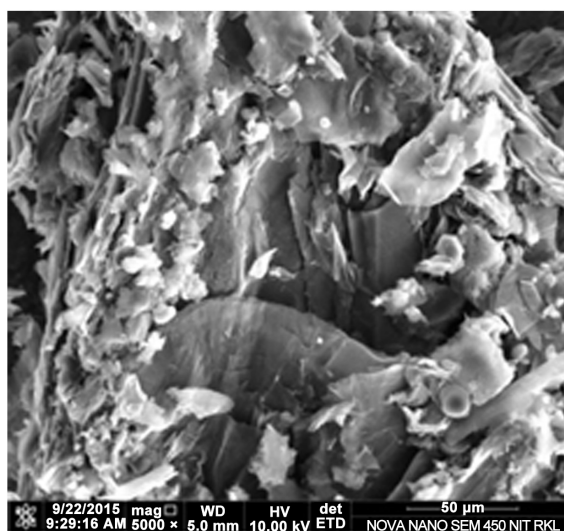
3. Results and Discussion Identify the Headings

Initially graphite oxide was prepared by oxidizing the purified natural flake graphite (NFG) by the modified Hummers method. Thereafter, graphene oxide (GO) was prepared by the exfoliation of the graphite oxide in distilled water in an ultrasonicator. GO was later reduced thermally to obtain reduced graphene oxide (rGO). **Figures 3(a)-(c)** are the SEM images of the as-received NFG. A modified Hummers method for synthesizing GO has been used here. Oxidation of the NFG results in a brown-colored viscous slurry. The slurry includes graphite oxide and exfoliated sheets along with non-oxidized graphitic particles and residual oxidizing agents. After repeated dialysis, salts and ions from the oxidation process are removed from the slurry. **Figure 4(b)** shows the GO sample that has been prepared in the present study. GO is brown in colour and shows yellow colour in relatively low concentrations. From the images in **Figure 4(b)** and **Figure 4(c)** it is evident that both NFG and rGO shows complete immiscibility in water. Both are found hydrophobic in nature. However, GO is readily miscible in water and gives a light brown solution when dissolved in water. The hydrophilicity of GO allows it to be uniformly deposited onto substrates in the form of thin films.

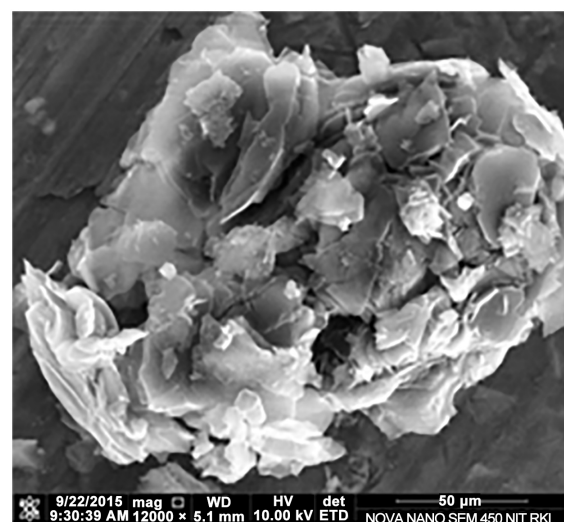
Figure 5(a) shows the XRD plot of the as-received NFG. From the XRD plot of the



(a)



(b)



(c)

Figure 3. (a)-(c) SEM images of as-received NFG.

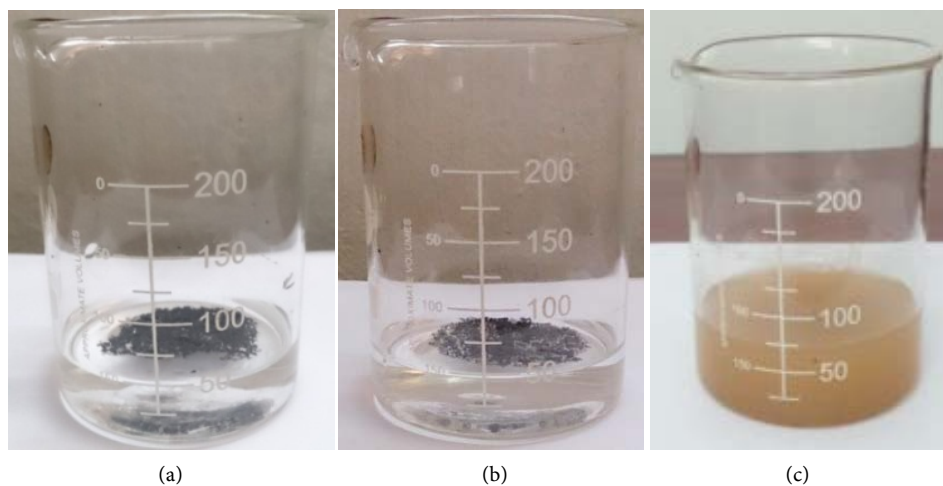


Figure 4. (a) NFG (hydrophobic); (b) GO (hydrophilic); and (c) rGO (hydrophobic) dispersed in water.

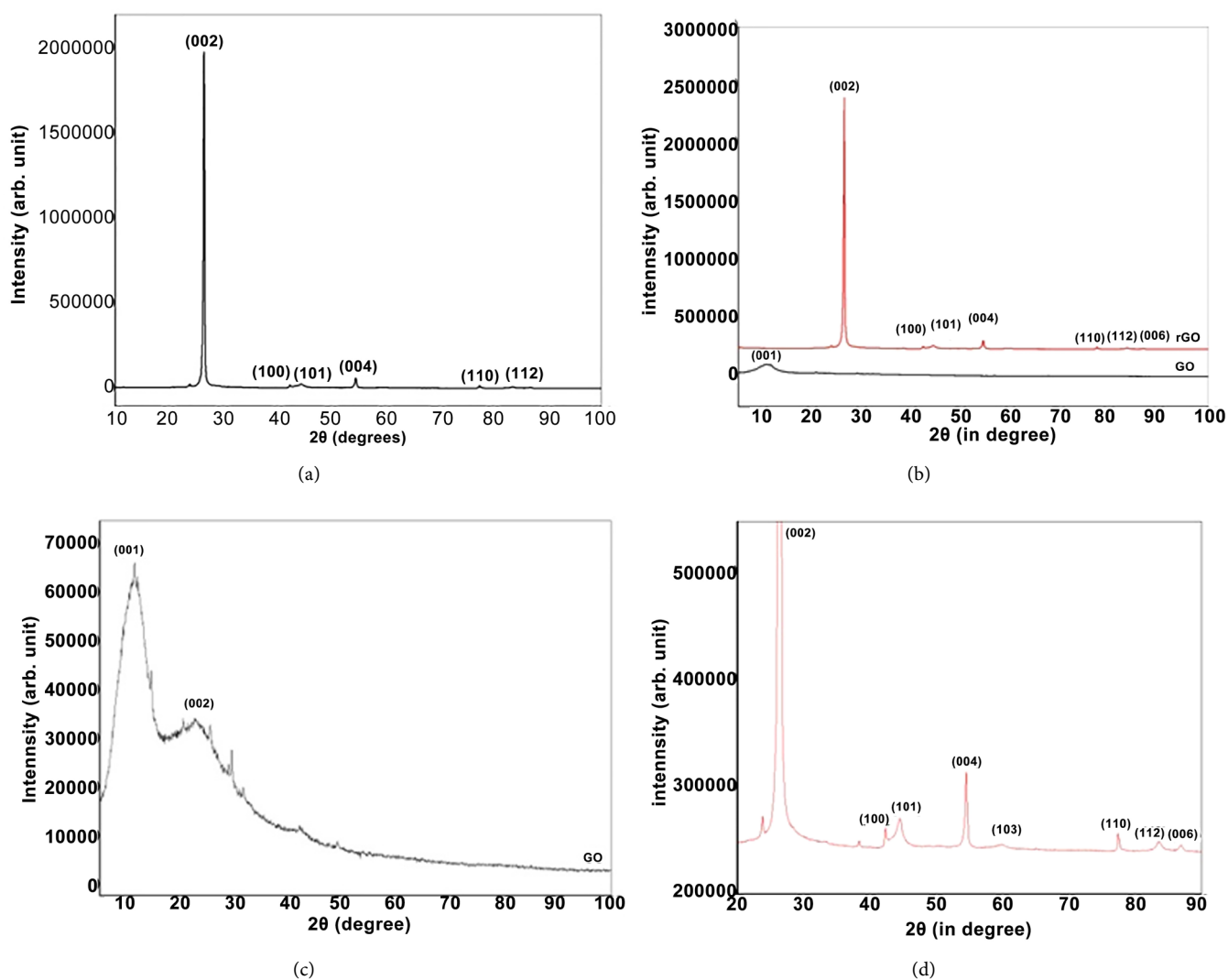


Figure 5. X-ray diffraction of (a) Natural flake graphite (NFG); (b) Comparison of the XRD plots of GO and rGO. XRD plots of (c) GO and (d) rGO.

as-received natural flake graphite in **Figure 1(a)**, it can be concluded that it is highly crystalline and has a very intense (002) peak at $2\theta = 26.42^\circ$ having a d-spacing of 3.37 \AA . **Figure 5(b)** shows the XRD plot of GO synthesized by modified Hummers method as well as rGO obtained from GO by thermal reduction. **Figure 5(b)** clearly shows the difference in the XRD patterns of GO and rGO. The XRD spectra of GO shows a sharp diffraction peak at $2\theta = 11.95^\circ$ with an interlayer distance of 7.4 \AA . The increase in interlayer spacing from 3.37 \AA in the case of NFG to about 7.4 \AA for GO is due to the introduction of the various functional groups that have been introduced by the oxidation of the NFG. The reduction of GO to graphene results in structural change as suggested by the comparison of the X-ray diffraction of GO and reduced GO or rGO. For rGO, the peak at 26.55° corresponds to the (002) diffraction plane with the interlayer spacing along the c-axis of 3.372 \AA . This spacing is slightly larger than that of the d spacing of bulk graphite (NFG). Besides the intense (002) peak, other low-intensity peaks corresponding to the (100), (101), (004) (110), (112) and (006) diffraction planes could also be seen in the XRD plot. The interlayer spacing was determined from the (002) peak by applying Bragg's law with a wavelength of $\text{Cu K}\alpha$ as 1.541 \AA . After the thermal treatment of GO at 350°C , the fact that the sharp diffraction peak at $2\theta = 11.95^\circ$ disappeared indicate the efficient exfoliation of the multiple layers during the thermal reduction of GO [22] [23] [24].

The SEM micrographs of GO synthesized by a modified Hummers processing **Figures 6(a)-(h)** clearly shows that the GO has a two-dimensional sheet-like structure. From the SEM images, it is evident that GO has a multiple lamellar layer structure and it is possible to distinguish the edges of individual sheets from the SEM images. The films are stacked one above the other and also show wrinkled areas. Lamellar structures having a length of upto 1.29 mm and width of $239\text{ }\mu\text{m}$ could be seen in the SEM images. The individual GO sheets were found to have a thickness of $1 - 2\text{ }\mu\text{m}$ and are found to be much larger than the thickness of single layer graphene. The increase in the thickness is due to the introduction of the oxygen-containing functional groups. It can also be noted that the GO sheets were thicker at the edges. This is because the oxygen-containing functional groups were mainly combined at the edges of GO. From the SEM images, it is evident that the GO sheets were firmly suspended and did not bend. From the EDX analysis in **Figure 6(f)**, it is evident that the GO contains around $65.52\text{ at.}\% \text{ C}$, $36.92\text{ at.}\% \text{ O}$ and $0.56\text{ at.}\% \text{ S}$. **Figures 6(i)-(k)** are the HRTEM images of GO and **Figures 6(l)** is the SAED pattern of the GO sample. The SAED pattern of GO reveals a spotty crystalline pattern [15] [19] [20].

GO can be reduced through several methods to obtain reduced graphene oxide (rGO). The SEM images of rGO obtained from GO in **Figure 7(a)** & **Figure 7(b)** demonstrate ultrathin graphene film obtained by the thermal reduction of GO. The SEM images suggest that rGO having a thickness less than $\sim 10\text{ nm}$ could be synthesized by this process. The EDX analysis suggests that the rGO sheets contain about $99.43\text{ at.}\% \text{ C}$ and $0.57\text{ at.}\% \text{ S}$. **Figure 7(c)** & **Figure 7(d)** are the HRTEM images of the rGO obtained by the thermal reduction of GO. **Figure 7(e)** is the SAD pattern obtained from the rGO sample. The AFM images in of GO in **Figure 8(a)** and rGO in **Figure 8(b)** clearly suggest that both the GO and rGO consists of few stacked layers [25] [26].

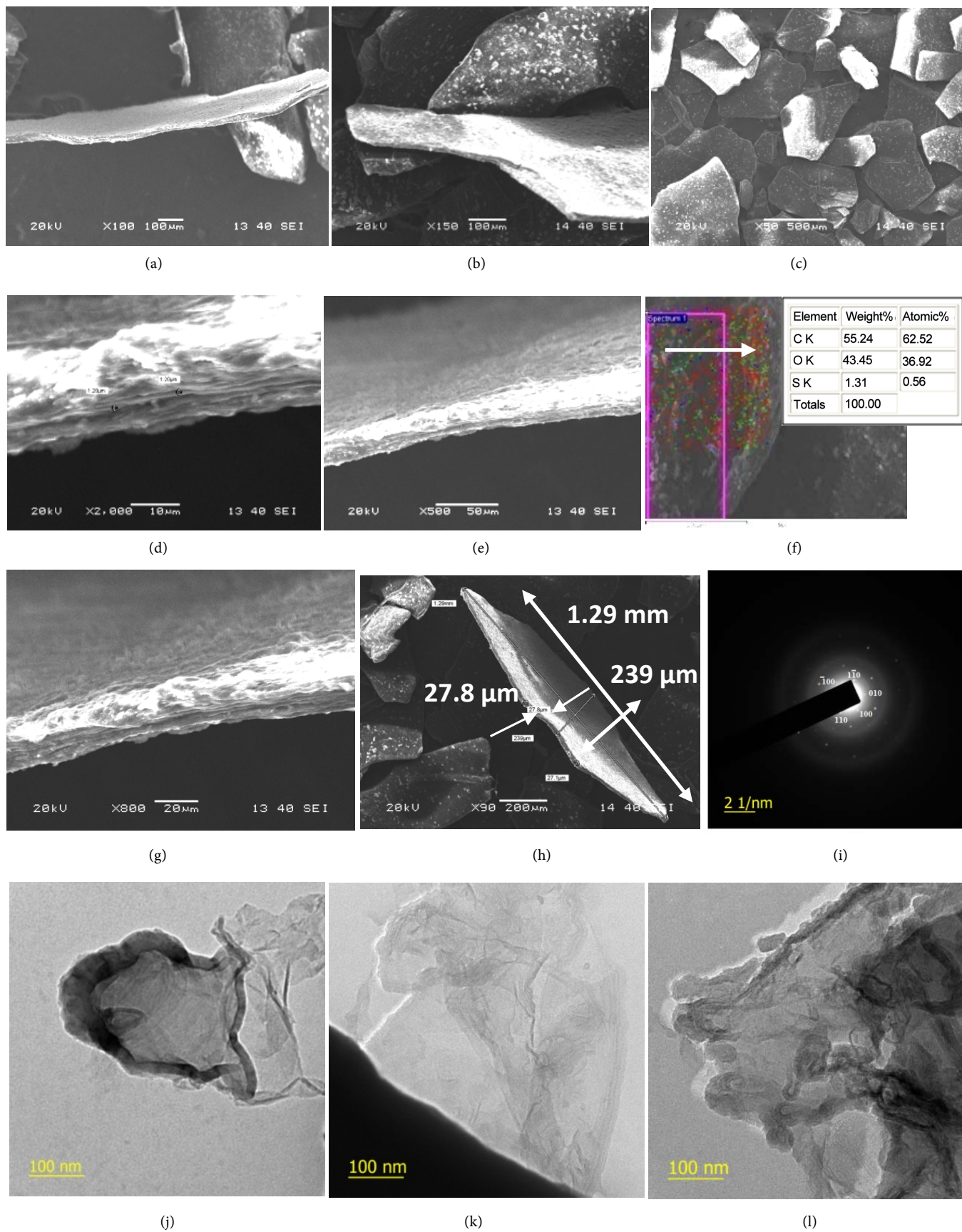


Figure 6. (a)-(h) SEM and EDX of GO; (i)-(k) HRTEM of GO; (l) SAED pattern of GO.

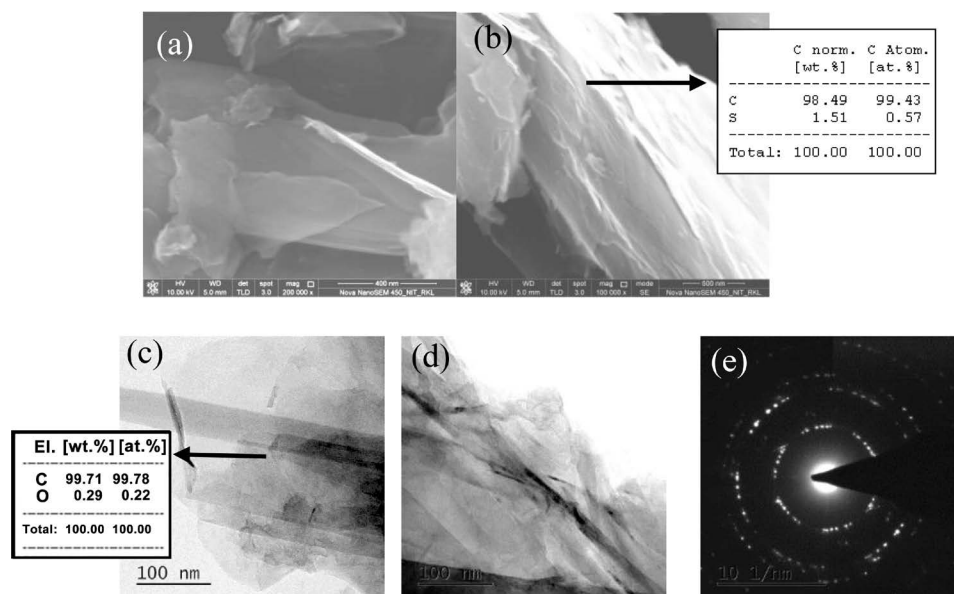
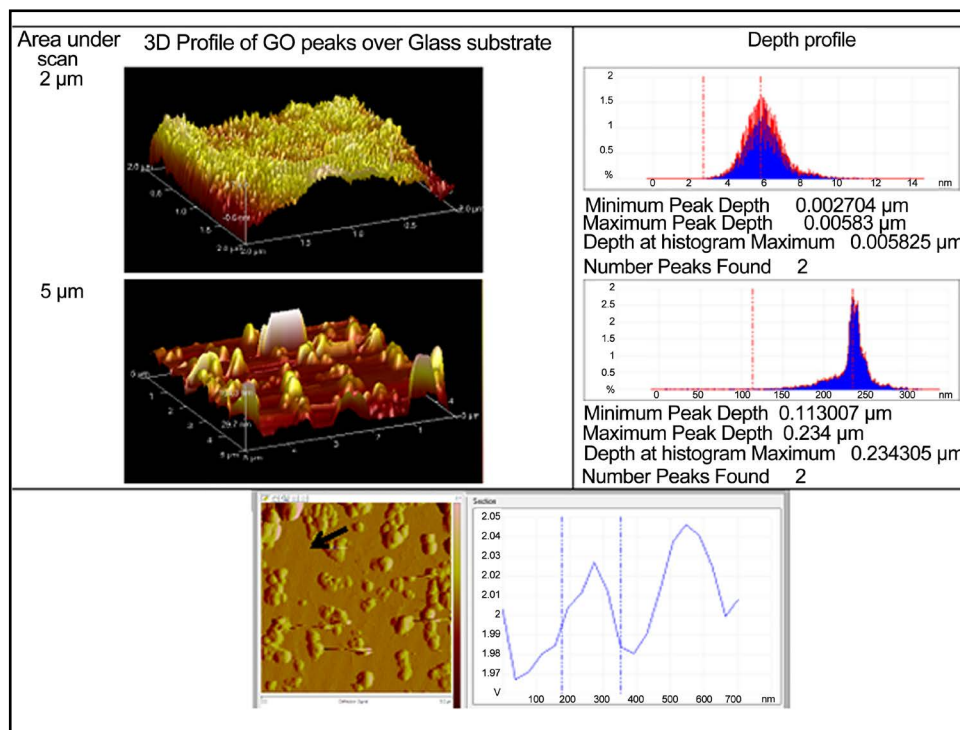


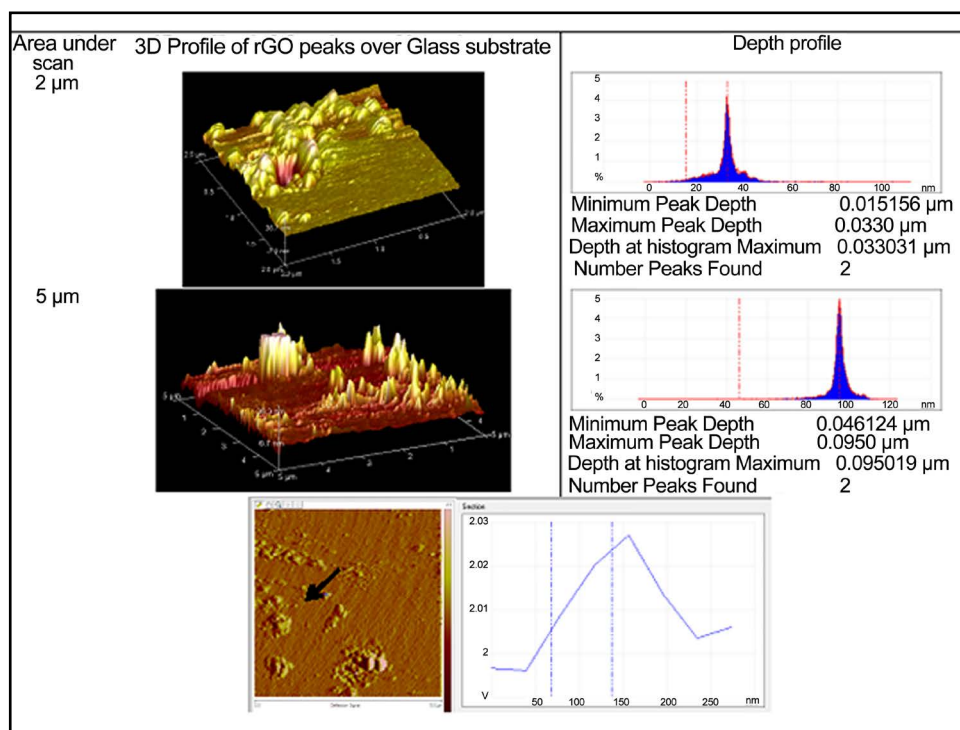
Figure 7. (a) (b) SEM images of rGO obtained from GO along with EDX analysis; (c) (d) HRTEM images; and (e) SAD pattern of rGO.

The DSC/TGA analysis was conducted to test the thermal stability of both GO and rGO. The DSC plot in **Figure 9(a)** shows a large exothermic peak at around 456°C. This exothermic peak corresponds to the combustion of the carbon skeleton of GO. A smaller exothermic peak is seen at around 212°C which corresponds to the evolution of CO and CO₂ from GO caused by the destruction of oxygenated functional groups. The TGA analysis of GO in **Figure 9(b)** indicates that the GO started to lose some mass below 100°C due to the evaporation of the adsorbed water and pyrolysis of oxygen-containing groups such as -OH, COOH, etc. The mass loss becomes very rapid as the temperature is raised. The TGA plot of GO suggests that the mass loss of GO takes place in three stages. About 20% mass loss occurred at the temperature of less than 100°C primarily due to the loss of H₂O molecules in GO. In the second stage, roughly 30% mass loss takes place occurring at a temperature of ~200°C due to the thermal decomposition of unstable oxygen-containing functional groups. This is due to the pyrolysis of oxygen-containing functional groups such as hydroxyl, carbonyl and carboxylic acid to yield CO, CO₂, and H₂O. Therefore, GO is expected to be effectively reduced into highly-conductive reduced GO (rGO) at around this temperature. Finally, a mass loss of about 40% occurred at 620°C mainly due to the combustion of the carbon backbone. At around 500°C the combustion of GO is complete. From the DSC and the TGA plot of rGO in **Figure 9(c)** and **Figure 9(d)** respectively it can be seen that the decomposition of the rGO sample starts at around 600°C and the decomposition is complete at around 800°C. The large exothermic peak at around 700°C is due to the sublimation of the carbon backbone. The onset decomposition temperature of rGO (~600°C) was much higher than that of GO. Comparison of the TGA analysis of GO in **Figure 9(b)** and that of rGO in **Figure 9(d)** it is evident that the GO sample decomposes in steps whereas, the rGO sample starts decomposing at a much later temperature and the decomposition are completed within ~600°C - 800°C. The lower starting temperature for rapid

mass loss in the case of the GO sample reflects the higher defect density present in the GO sample. Lower defect density results in higher thermal stability in the case of the rGO sample [26] [27].



(a)



(b)

Figure 8. AFM of (a) GO and (b) rGO.

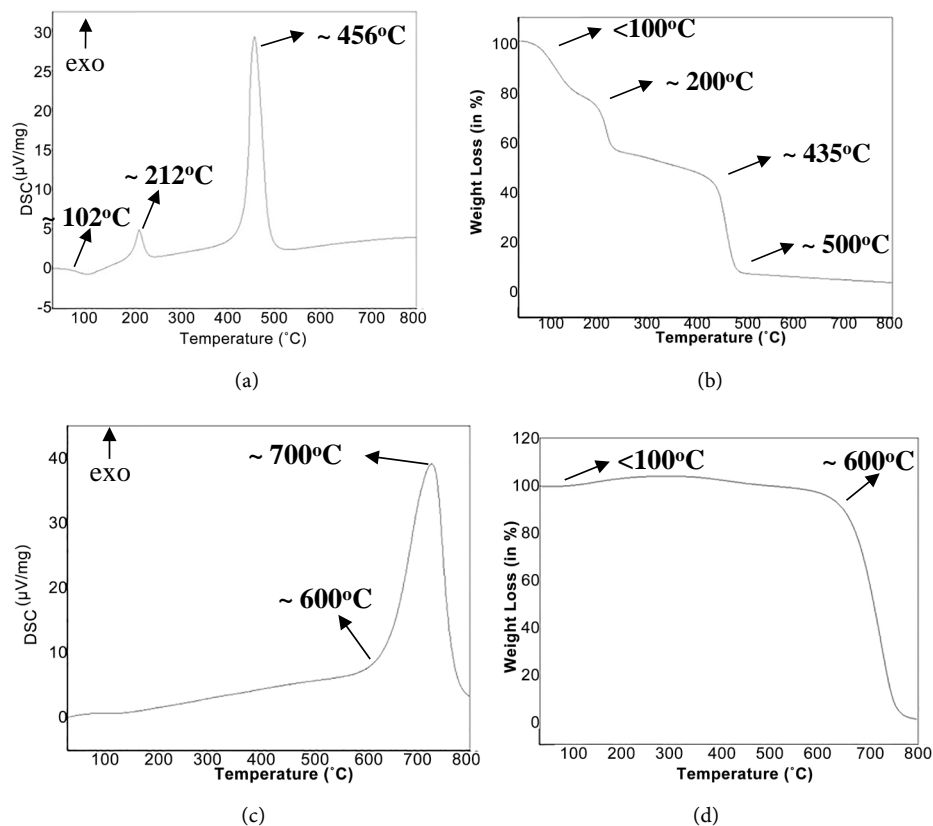


Figure 9. (a) DSC and (b) TGA of GO; (c) DSC and (d) TGA of rGO.

Raman spectroscopy is a non-destructive technique which is a widely used tool to obtain structural information of carbon-based materials. The main features in the Raman spectra of graphitic carbon-based materials are the G and D peaks and their overtones. **Figure 10(a)** is the Raman spectra of as-received NFG sample. The two most intense peaks are the G band at 1580 cm^{-1} and the 2D band at 2700 cm^{-1} . The G peak is due to the bond stretching of all pairs of sp_2 atoms in both the rings and chains. It is the result of in-plane optical vibrations and corresponds to the optical E_{2g} phonons at the Brillouin zone center resulting from the bond stretching of sp_2 carbon pairs in both, rings and chains. The 2D band, also known as the G' band, is the second most prominent band in the Raman spectra and is always observed in graphite samples. The peak at 1350 cm^{-1} is also called the D peak and reveals defects in the sample. The D peak is due to first order resonance. The D peak represents the breathing mode of aromatic rings arising due to the defects in the sample. The D-peak intensity is therefore often used as a measure of the degree of disorder. The Raman spectra of GO in **Figure 10(b)** shows the presence of a very strong D peak at $\sim 1350\text{ cm}^{-1}$ with an intensity comparable to that of the G peak at $\sim 1580\text{ cm}^{-1}$. The intense D peak along with a large bandwidth suggest the significant structural disorder in GO. The 2D peak at around 2680 cm^{-1} is attributed to double resonance transitions resulting in the production of two phonons with opposite momentum. Unlike the D peak, which is Raman active only in the presence of defects, the 2D peak is active even in the absence of any defects. A defect-activated peak called D + G is also visible at around 2950 cm^{-1} [28] [29]. FTIR spectroscopy

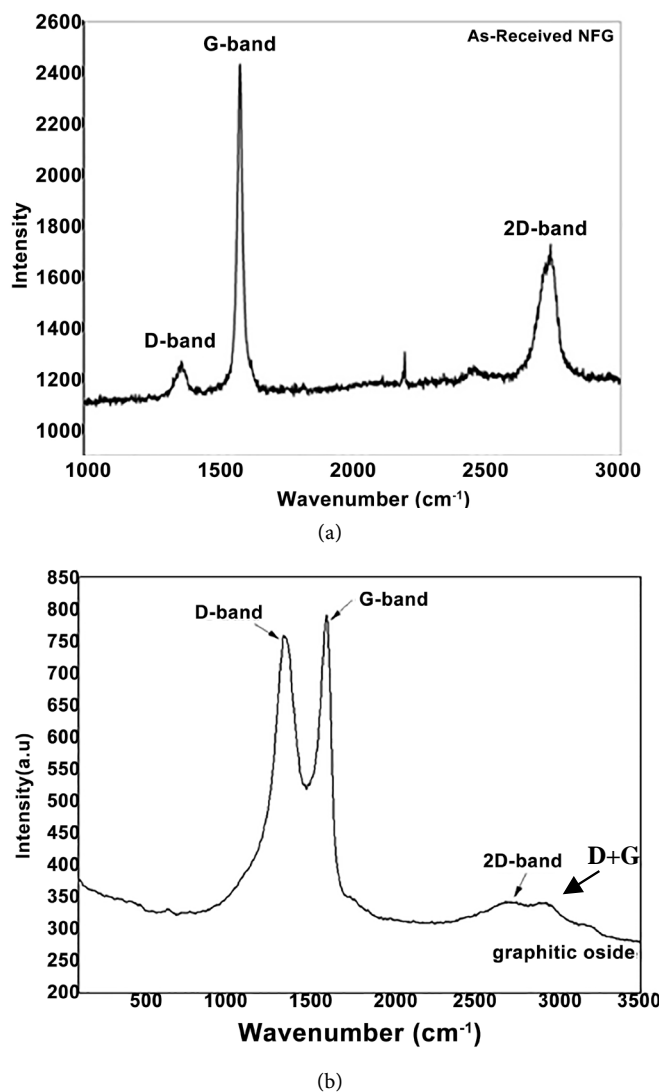


Figure 10. Raman spectra of as received (a) NFG and (b) GO.

analysis was done in order to investigate the structure and functional groups in NFG, GO, and rGO. The FTIR spectrum of GO in **Figure 11(b)** shows a broad peak between $3000 - 3700 \text{ cm}^{-1}$ in the high-frequency area corresponding to the stretching and bending vibration of OH groups of water molecules adsorbed on GO. Therefore, it can be concluded that the sample has strong hydrophilicity. For GO, the characteristic peaks for carboxyl C=O were seen at 1735 cm^{-1} . By comparison of the FTIR spectra of GO and rGO in **Figure 11(b)** and **Figure 11(c)** respectively it is evident that the characteristic peak for carboxyl C=O at 1735 cm^{-1} showed a much lower intensity for rGO. After the thermal treatment at 300°C for the rGO sample, the peaks for oxygen functional groups were reduced significantly. The peak at 1573 cm^{-1} attributed to the aromatic C=C group could be seen in both GO and rGO samples. The comparison of the FTIR spectra from both the samples suggests that the thermal treatment is very effective in reducing GO to form rGO. The presence of the absorption peak observed in the medium frequency area in the spectrum of both GO and rGO, at 1630 cm^{-1} can be attributed to the stretching vibration of C=C. The presence of these oxygen-containing

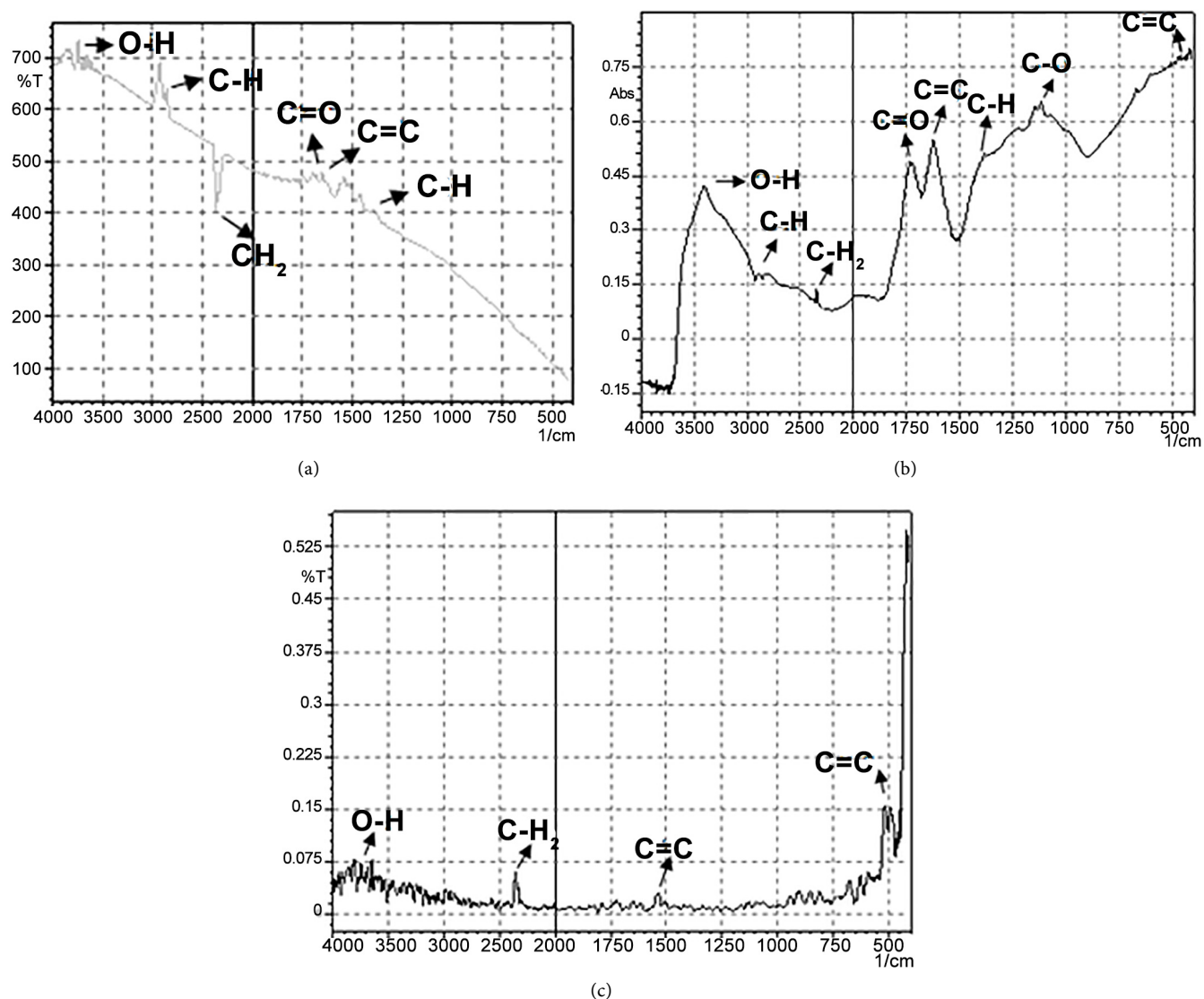


Figure 11. FTIR of (a) NFG; (b) GO; (c) rGO.

groups reveals that the graphite has been oxidized. The polar groups, especially the surface hydroxyl groups, result in the formation of hydrogen bonds between graphite and water molecules. This results in the hydrophilic nature of graphene. In the case of rGO a reduction in the intensity of the aromatic C=C (1622 cm^{-1}), carboxyl C-O (1414 cm^{-1}), and C-O (1116 cm^{-1}) could be seen. The absorption peaks at 1110 cm^{-1} seen in the FTIR spectra of GO in **Figure 10(b)** corresponds to the stretching vibration of C-O [29] [30].

The BET analysis suggests that GO has an area of $8.821\text{ m}^2/\text{g}$. It has a total pore volume of 0.1668 cc/g and the average pore diameter is 3407.1 \AA . The particle size distribution analysis in **Figure 12** shows that the rGO has a slightly lower size than the GO. Around 20 vol.% of the GO particles were found to have a size of 1796 nm whereas about 23 vol.% of the rGO powder particles were found to have a particle size of 702.9 nm . The UV-vis spectra of aqueous GO, rGO, and NFG dispersions are shown in **Figure 13**. Two kinds of characteristic features can be observed in the spectra. A shoulder

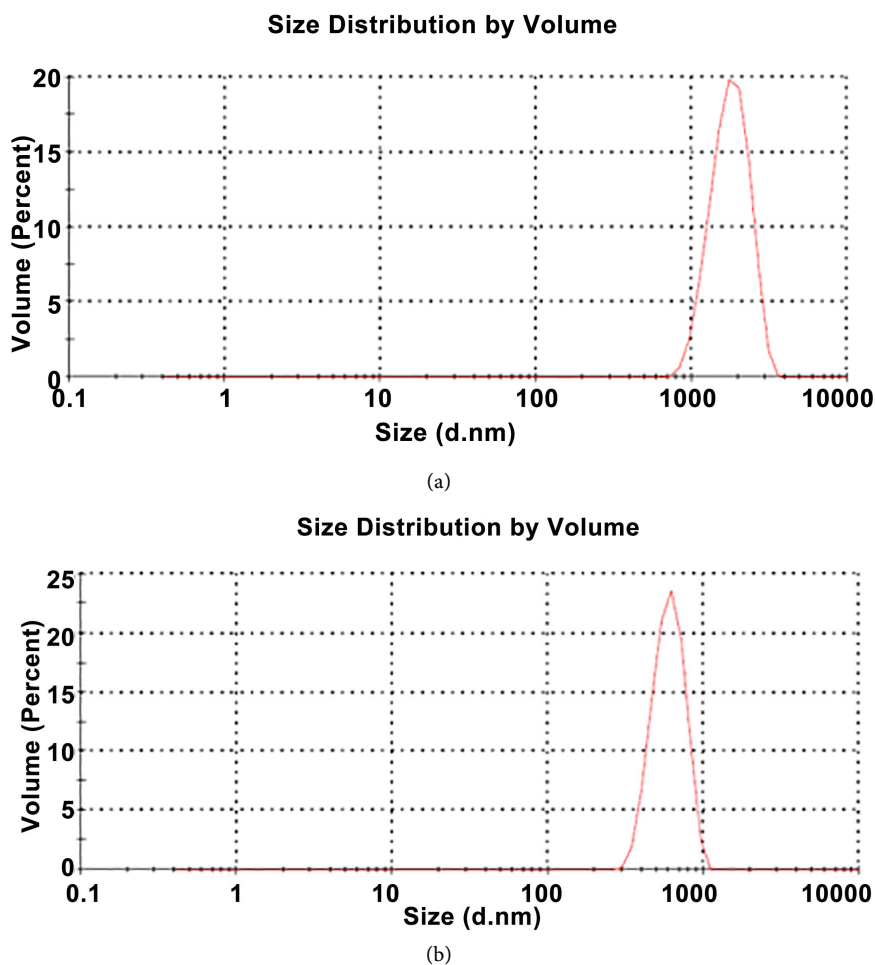


Figure 12. Particle size distribution analysis of (a) GO and (b) rGO.

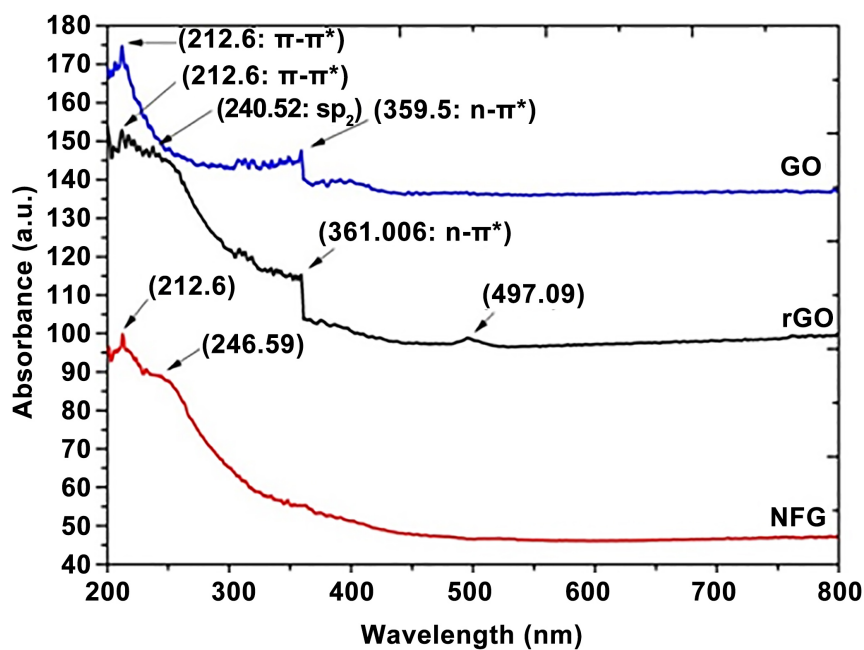


Figure 13. UV-vis spectra of aqueous dispersions of NFG, rGO, and GO.

at ~359 nm could be seen which corresponds to the $n-\pi^*$ plasmon peak. A similar shoulder could also be seen in the case of rGO. The second characteristic feature appears at approximately 212.6 nm and corresponds to a $\pi-\pi^*$ transition of the aromatic C-C bonds which corresponds to the sp^3 character in GO which later transforms to a significant shoulder at around 240 nm in the case of rGO which clearly visualizes the absorbance by sp^2 hybrids of rGO [31].

4. Conclusion

Graphene oxide (GO) was successfully prepared by oxidizing purified natural flake graphite (NFG) by a modified Hummer's method. GO was later thermally reduced to synthesize reduced GO (rGO). The GO synthesized by the modified Hummer's method was found to consist of stacks of GO sheets. These stacks were found to have a thickness of about 1 - 2 μm . The GO sheets were also thicker at the edges due to the oxygen-containing functional groups attached at the edges of GO. The hydrophilicity of GO allows it to be readily dissolved in solvents like water whereas both natural flake graphite and the rGO were found to be hydrophobic in nature. Thermal analysis results indicate that rGO has higher thermal stability as compared to GO due to lower defect density. The comparison of the FTIR spectra from both the samples suggests that the thermal treatment is very effective in reducing GO to form rGO. A comparison of the particle size distribution of rGO and GO suggests that rGO has a lower average particle size as compared to GO.

Acknowledgements

We gratefully acknowledge the support provided by the XRD, SEM, and thermal analysis laboratories of Metallurgical and Materials Engineering Department and the FESEM laboratory of the Ceramic Engineering Department, NIT Rourkela. We also thank the support provided by Chemistry Department, NIT Rourkela. We would also like to acknowledge Central Research Facility, IIT Kharagpur for helping us in Raman spectroscopy analysis of the samples.

References

- [1] Geim, A.K. and Novoselov, K.S. (2007) The Rise of Graphene. *Nature Materials*, **6**, 183-191. <https://doi.org/10.1038/nmat1849>
- [2] Saxena, S. and Tyson, A. (2010) Interacting Quasi-Two-Dimensional Sheets of Interlinked Carbon Nanotubes: A High-Pressure Phase of Carbon. *ACS Nano*, **4**, 3515-3521. <https://doi.org/10.1021/nn100626z>
- [3] Novoselov, K.S., Geim, A.K., Morozov, S.V., Jiang, D., Zhang, Y., Dubonos, S.V., Grigorieva, I.V. and Firsov, A.A. (2004) Electric Field Effect in Atomically Thin Carbon Films. *Science*, **306**, 666-669. <https://doi.org/10.1126/science.1102896>
- [4] Berger, C., Song, Z., Li, X., Wu, X., Brown, N., Naud, C., Mayou, D., Li, T., Hass, J., Marchenkov, A.N., Conrad, E.H., First, P.N. and De Heer, W.A. (2006) Electronic Confinement and Coherence in Patterned Epitaxial Graphene. *Science*, **312**, 1191-1196. <https://doi.org/10.1126/science.1125925>
- [5] Higginbotham, A.L., Lomeda, J.R., Morgan, A.B. and Tour, J.M. (2009) Graphite Oxide Flame Retardant Polymer Nanocomposites. *Applied Material Interfaces*, **1**, 2256-2261. <https://doi.org/10.1021/am900419m>

- [6] Lerf, A., He, H., Forster, M. and Klinowski, J. (1998) Structure of Graphite Oxide Revisited. *Journal of Physical Chemistry B*, **102**, 4477-4482. <https://doi.org/10.1021/jp9731821>
- [7] Ruoff, R. (2008) Graphene Calling All Chemists. *Nature Nanotechnology*, **3**, 10-11. <https://doi.org/10.1038/nnano.2007.432>
- [8] He, H., Klinowski, J. and Forster, M. (1998) A New Structural Model for Graphite Oxide. *Chemical Physics Letters*, **287**, 53-56. [https://doi.org/10.1016/S0009-2614\(98\)00144-4](https://doi.org/10.1016/S0009-2614(98)00144-4)
- [9] Uhl, F. and Wilkie, C. (2004) Preparation of Nanocomposites from Styrene and Modified Graphite Oxides. *Polymer Degradation and Stability*, **84**, 215-226. <https://doi.org/10.1016/j.polymdegradstab.2003.10.014>
- [10] Hontoria-Lucas, C., Lopez Peinado, A., Lopez Gonzalez, J., Rojas Cervantes, M. and Martin-Aranda, R. (1995) Study of Oxygen Containing Groups in a Series of Graphite Oxides: Physical and Chemical Characterization. *Carbon*, **33**, 1585-1592. [https://doi.org/10.1016/0008-6223\(95\)00120-3](https://doi.org/10.1016/0008-6223(95)00120-3)
- [11] Brodie, B.C. (1859) On the Atomic Weight of Graphite. *Philosophical Transactions of the Royal Society of London*, **149**, 249-259. <https://doi.org/10.1098/rstl.1859.0013>
- [12] Staudenmaier, L. (1898) Verfahren zur Darstellung der Graphitsaure. *Berichte der Deutschen Chemischen Gesellschaft*, **31**, 1481-1487. <https://doi.org/10.1002/cber.18980310237>
- [13] Hummers, W.S. and Offeman, R.E. (1958) Preparation of Graphitic Oxide. *Journal of The American Chemical Society*, **80**, 1339. <https://doi.org/10.1021/ja01539a017>
- [14] Ishikawa, T. and Nagaoki, T. (1986) Shin tanso kogyo (New Carbon Industry). 2nd Edition, Kindai Hensyusya, Tokyo, 125-136.
- [15] Pei, S. and Cheng, H.M. (2012) The Reduction of Graphene Oxide. *Carbon*, **50**, 3210-3228. <https://doi.org/10.1016/j.carbon.2011.11.010>
- [16] Ramakrishnan, M.C. and Thangavelu, R.R. (2013) Synthesis and Characterization of Reduced Graphene Oxide. *Advanced Materials Research*, **678**, 56-60. <https://doi.org/10.4028/www.scientific.net/AMR.678.56>
- [17] Stobinski, L., Lesiak, B., Malolepszy, A., Mazurkiewicz, M., Mierzwa, B., Zemek, J., Jiricek, P. and Bieloshapka, I. (2014) Graphene Oxide and Reduced Graphene Oxide Studied by the XRD, TEM and Electron Spectroscopy Methods. *Journal of Electron Spectroscopy and Related Phenomenon*, **195**, 145-154. <https://doi.org/10.1016/j.elspec.2014.07.003>
- [18] Marcano, D.C., Kosynkin, D.V., Berlin, J.M., Sinitskii, A., Sun, Z., Slesarev, A., Alemany, L.B., Lu, W. and Tour, J.M. (2010) Improved Synthesis of Graphene Oxide. *ACS Nano*, **4**, 4806-4814. <https://doi.org/10.1021/nn1006368>
- [19] Fu, C., Zhao, G., Zhang, H. and Li, S. (2013) Evaluation and Characterization of Reduced Graphene Oxide Nanosheets as Anode Materials for Lithium-Ion Batteries. *International Journal of Electrochemical Science*, **8**, 6269-6280.
- [20] Stankovich, S., Dikin, D., Piner, R.D., Kohlhaas, K.A., Kleinhammes, A., Jia, Y., Wu, Y., Nguyen, S.B.T. and Ruoff, R.S. (2007) Synthesis of Graphene-Based Nanosheets via Chemical Reduction of Exfoliated Graphite Oxide. *Carbon*, **45**, 1558-1565. <https://doi.org/10.1016/j.carbon.2007.02.034>
- [21] Wang, G., Yang, J., Park, J., Gou, X., Wang, B., Liu, H. and Yao, J. (2008) Facile Synthesis and Characterization of Graphene Nanosheets. *The Journal of Physical Chemistry C*, **112**, 8192-8195. <https://doi.org/10.1021/jp710931h>
- [22] Nasrollahzadeh, M., Babaei, F., Fakhriand, P. and Jaleh, B. (2015) Synthesis, Characterization, Structural, Optical Properties and Catalytic Activity of Reduced Graphene Oxide/Copper Nanocomposites. *RSC Advance*, **5**, 10782-10789. <https://doi.org/10.1039/C4RA12552E>
- [23] Ju, H.M., Choi, S.H. and Huh, S.H. (2010) X-Ray Diffraction Patterns of Thermally-Reduced Graphenes. *Journal of the Korean Physical Society*, **57**, 1649-1652.

- <https://doi.org/10.3938/jkps.57.1649>
- [24] Chen, J., Yao, B., Li, C. and Shi, G. (2013) An Improved Hummers Method for Eco-Friendly Synthesis of Graphene Oxide. *Carbon*, **64**, 225-229. <https://doi.org/10.1016/j.carbon.2013.07.055>
- [25] Guo, H.L., Wang, X.F., Qian, Q.Y., Wang, F. and Xia, X.H. (2009) A Green Approach to the Synthesis of Graphene Nanosheets. *ACS Nano*, **3**, 2653-2659. <https://doi.org/10.1021/nn900227d>
- [26] Malas, A., Das, C.K., Das, A. and Heinrich, G. (2012) Development of Expanded Graphite Filled Natural Rubber Vulcanizates in Presence and Absence of Carbon Black: Mechanical, Thermal and Morphological Properties. *Materials and Design*, **39**, 410-417. <https://doi.org/10.1016/j.matdes.2012.03.007>
- [27] Zhang, S.T., Gu, A.Y., Gao, H.F. and Che, X.Q. (2011) Characterization of Exfoliated Graphite Prepared with the Method of Secondary Intervening. *International Journal of Industrial Chemistry*, **2**, 123-130.
- [28] Zhu, Y., Murali, S., Cai, W., Li, X., Suk, J.W., Potts, J.R. and Ruoff, R.S. (2010) Graphene and Graphene Oxide: Synthesis, Properties, and Applications. *Advanced Materials*, **22**, 3906-3924. <https://doi.org/10.1002/adma.201001068>
- [29] Shahriary, L. and Athawale, A.A. (2014) Graphene Oxide Synthesized by Using Modified Hummers Approach. *International Journal of Renewable Energy and Environmental Engineering*, **2**, 58-63.
- [30] Bykkam, S., Rao, V.K., Chakra, C.H.S. and Thunugunta, T. (2013) Synthesis and Characterization of Graphene Oxide and Its Antimicrobial Activity against *Klebsiella* and *Staphylococcus*. *International Journal of Advanced Biotechnology and Research*, **4**, 142-146.
- [31] Lai, Q., Zhu, S., Luo, X., Zou, M. and Huang, S. (2012) Ultraviolet-Visible Spectroscopy of Graphene Oxides. *AIP Advances*, **2**, Article ID: 032146. <https://doi.org/10.1063/1.4747817>



Submit or recommend next manuscript to SCIRP and we will provide best service for you:

Accepting pre-submission inquiries through Email, Facebook, LinkedIn, Twitter, etc.

A wide selection of journals (inclusive of 9 subjects, more than 200 journals)

Providing 24-hour high-quality service

User-friendly online submission system

Fair and swift peer-review system

Efficient typesetting and proofreading procedure

Display of the result of downloads and visits, as well as the number of cited articles

Maximum dissemination of your research work

Submit your manuscript at: <http://papersubmission.scirp.org/>

Or contact graphene@scirp.org